arXiv:2109.03090v2 [cond-mat.mes-hall] 8 Sep 2021

Experimental verification of the work fluctuation-dissipation relation for information-to-work conversion

David Barker,[1] Matteo Scandi,[2] Sebastian Lehmann,[1] Claes Thelander,[1]
Kimberly A. Dick,[1,3] Martí Perarnau-Llobet,[4] and Ville F. Maisi[1]

[1] *NanoLund and Solid State Physics, Lund University, Box 118, 22100 Lund, Sweden*
[2] *ICFO - Institut de Ciencies Fotoniques, The Barcelona Institute of Science and Technology, Castelldefels (Barcelona), 08860, Spain*
[3] *Centre for Analysis and Synthesis, Lund University, Box 124, 22100 Lund, Sweden.*
[4] *Département de Physique Appliquée, Université de Genéve, Genéve, Switzerland*

(Dated: January 13, 2022)

We study experimentally work fluctuations in a Szilard engine that extracts work from information encoded as the occupancy of an electron level in a semiconductor quantum dot. We show that as the average work extracted per bit of information increases towards the Landauer limit $k_BT\ln 2$, the work fluctuations decrease in accordance with the work fluctuation-dissipation relation. We compare the results to a protocol without measurement and feedback and show that when no information is used, the work output and fluctuations vanish simultaneously contrasting the information-to-energy conversion case where increasing amount of work is produced with decreasing fluctuations. Our work highlights the importance of fluctuations in the design of information-to-work conversion processes.

When considering thermodynamic processes at the microscale, where thermal and quantum fluctuations play a dominant role, one faces the challenge of describing work and heat as stochastic quantities. Understanding and characterising their statistics has become an active area of research, and is one of the main aims of the fields of stochastic and quantum thermodynamics [1–5]. The exact form of heat and work distributions highly depends on the specific protocol in question. The situation considerably simplifies when considering finite-time processes where the system remains close to the instantaneous equilibrium state (i.e., in the linear-response regime with respect to the driving speed) [6–14]. In this case, and when no quantum coherence is generated along the process, the work distribution takes a Gaussian shape [7, 9, 13], with its first and second moments related through the work fluctuation-dissipation relation (FDR) [15–18]:

$$W_{diss} = \frac{1}{2k_BT}\sigma_W^2. \tag{1}$$

Here, T is the temperature of the surrounding environment, k_B is Boltzmann's constant, $W_{\rm diss}$ is the average dissipated work along the process:

$$W_{diss} := \langle W\rangle - \Delta F, \tag{2}$$

i.e., the difference between the mean work $\langle W\rangle$ performed to the system and the change in equilibrium free energy ΔF, and finally σ_W^2 is the variance of the work distribution. The work FDR is a central result in stochastic thermodynamics: it implies that near equilibrium dissipation comes inevitably accompanied by fluctuations, and conversely that optimal protocols minimising dissipation will automatically also minimise fluctuations [8, 19]. The FDR also plays a crucial role in the estimation of equilibrium free energy differences through measurements of non-equilibrium processes [20, 21].

The main goal of this article is to experimentally validate the fundamental relation Eq. (1) by using an electronic system. For that, we consider one of the most relevant thermodynamic processes at the nanoscale: the conversion of information into work. Inspired by the Szilard engine, we implement an information engine which uses one bit of information (an extra electron being located on the quantum dot or not) to extract work $W_{\rm ex} \equiv -W$ from a thermal reservoir at temperature T. This cycle and its inverse, the so-called Landauer erasure, has been extensively studied in the literature, both theoretically [22–33] and experimentally [34–39]. It is well known that the average extractable work is bounded by $\langle W_{\rm ex}\rangle \leq k_BT\ln 2$, which can only be reached for infinitesimally slow processes –the so-called Landauer limit. Previous experimental influential works have successfully managed to approach this limit to a high degree in various platforms at the level of average work [34–39]. In contrast, here we focus our attention on the behaviour of work fluctuations, and in particular show how Eq. (1) is satisfied as the Landauer limit is approached. As predicted from the FDR, our results clearly demonstrate a decrease in work fluctuations as the dissipation is minimised by increasing the operation cycle time of the engine. Therefore, the information about the electron's position can be exploited to extract work in an almost-deterministic fashion. To contrast this information-to-work process, we consider a cyclic process where no information on the electron's position is available. In this case, we also observe that both work fluctuations and dissipation decrease according to (1) as the operating time of the cycle increases. However, the average extracted work always remains negative, $\langle W_{\rm ext}\rangle \leq 0$ and approaches zero for long cycle times, in agreement with the second law of thermodynamics. This contrasts the information engine that provides a positive finite work output with fluctuations vanishing towards long cycle times.

Our device is based on a semiconductor quantum dot which allows for the manipulation of discrete energy levels as opposed to the metallic system used in Ref 38. This work thus provides an experimental insight into the nature of thermodynamic fluctuations in nanoscale systems as well as an alternative platform to study information-to-work conversion with high efficiency.

Set-up. Our device is shown in Figure 1a). It consists of a quantum dot (QD) system formed with polytypes in an InAs nanowire [40–43]. The bit of information we use in our experiment is encoded in the occupancy of an electronic state in the leftmost QD (QD1). The state is at discrete energy level E which we drive using the plunger gate voltage V_{g1} with the lever arm $\alpha = 1.7 \times 10^4 k_B T/\mathrm{V}$. The rightmost QD is voltage biased with V_b and used as an electrometer which detects the occupancy n of the state [44, 45] through the current I_d as shown in Figure 1b). Meanwhile, the middle QD is put in Coulomb blockade allowing tunneling from QD1 only to the left electronic reservoir. As in Refs. 38, 46, 47, our experiment is performed in a regime where $n \in \{0, 1\}$ (i.e., the QD1 has an extra electron or not). n switches whenever an electron tunnels between QD1 and the left-most fermionic reservoir at temperature $T = 100\,\mathrm{mK}$, given by the cryostat temperature. The tunneling occurs with the rates $\Gamma_{\mathrm{in}} = \Gamma_0(1 + bE)f(E)$ and $\Gamma_{\mathrm{out}} = 2\Gamma_0(1+bE)(1-f(E))$ where $\Gamma_0 = 64\,\mathrm{Hz}$ and $b = 0.025/k_B T$ were determined using a feedback protocol developed in Ref 48, and $f(E) = 1/(1 + e^{\beta(E)})$ is the Fermi-Dirac distribution. The average occupancy $p(t)$ of the QD state is then governed by the rate equation:

$$\dot{p}(t) = \Gamma_{\mathrm{in}}(1 - p(t)) - \Gamma_{\mathrm{out}}\, p(t). \tag{3}$$

Finite-time thermodynamics and work fluctuation-dissipation relation. In the experiment, we consider protocols where the energy $E(t)$ is driven linearly from $E(0) \equiv E_i$ to $E(\tau) \equiv E_f$ for a time τ. Work W is performed on the system whenever $n(t) = 1$ during the drive, i.e., $W \equiv \int_0^\tau \mathrm{d}t\, n(t)\dot{E}(t)$. Note that work is a stochastic quantity due to fluctuations in $n(t)$ [1–5]. Sufficient repetitions of the protocol enables us to obtain the work probability distribution $P(W)$ experimentally. Its first moment is given by $\langle W\rangle = \int_0^\tau \mathrm{d}t\, p(t)\dot{E}(t)$, and we refer to the second moment as σ_W^2.

The average work can be decomposed into a reversible and irreversible contribution: $\langle W\rangle = \Delta F + W_{\mathrm{diss}}$ [1–5]. Here, ΔF is the change of equilibrium free energy:

$$\Delta F \equiv \int_0^\tau \mathrm{d}t\, p^{\mathrm{eq}}(t)\dot{E}(t) = \frac{1}{\beta}\ln\left(\frac{\mathcal{Z}_i}{\mathcal{Z}_f}\right), \tag{4}$$

where $p^{\mathrm{eq}}(t) = 1/(1 + 2e^{\beta E(t)})$ is the instantaneous equilibrium state, and $\mathcal{Z}_x = 1 + 2e^{-\beta E_x}$ with $x = i, f$. The dissipated work W_{diss} is instead given by (see Appendix for a detailed derivation):

$$W_{\mathrm{diss}} = \beta\int_0^\tau \mathrm{d}t\, [1 - p^{\mathrm{eq}}(t)]p^{\mathrm{eq}}(t)\frac{\dot{E}(t)^2}{\Gamma(t)} + \mathcal{O}\left(\frac{1}{\tau\Gamma_0}\right)^2 \tag{5}$$

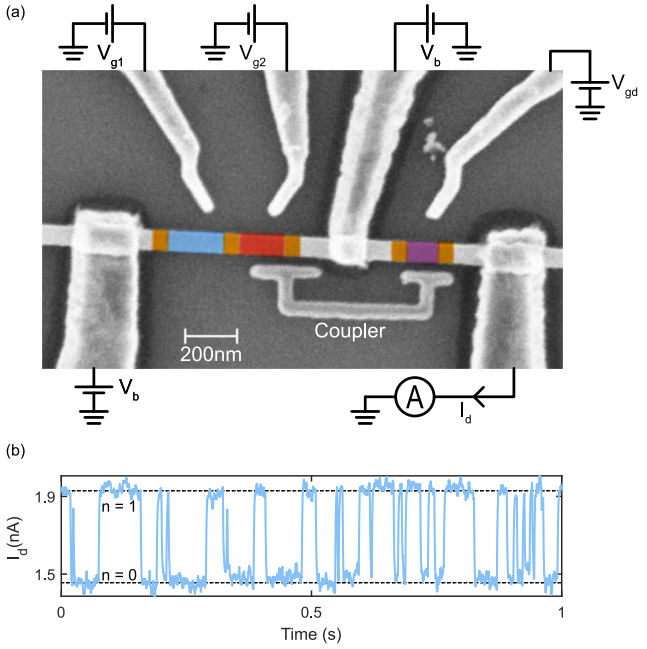


FIG. 1. a) Scanning electron microscope image of the nanowire device. Embedded in the nanowire are three QDs, each aligned to one of the plunger gates V_{g1},V_{g2} or V_{gd}. Contacts separate the device into one part with two QDs and one part with a single QD. The coupler couples the two systems together, allowing the current I_d through the lone QD to provide a measure of the charge state of the other system. Here, the QD involved in the experiment is marked in blue (close to the plunger gate with V_{g1}) while the quantum dot marked in red is put in Coulomb blockade. The sensor QD is marked in purple and the tunnel barriers are coloured orange. b) An example of the sensor current I_d at the start of the experiment. V_{gd} is set so that a high current represents the state $n = 1$ and V_{g1} is set so that the average $\langle n\rangle = 0.5$.

where we have introduced $\Gamma(t) = \Gamma_0(1 + bE(t))$. In Eq. (5) we have neglected contributions of order $(\tau\Gamma_0)^{-2}$, which is well justified in the experiment for $\tau \gtrsim 1$ s (for $\tau = 1$ s we have: $1/\tau\Gamma_0 \approx 0.16$). On the other hand, in the Appendix, we show that work fluctuations satisfy: $\sigma_w^2 = 2W_{\mathrm{diss}}/\beta + \mathcal{O}(\Gamma_0\tau)^{-2}$. That is, the FDR is satisfied at order $1/\tau\Gamma_0$, which is in agreement with the more general considerations of Refs. 17 and 18. The regime where W_{diss} (and σ_w^2) decay with $1/\tau$ is often known in the literature as the low-dissipation regime, see e.g. Refs. 49–54.

Information-to-work conversion. The device is operated as a Szilard engine and extracts work using the protocol developed in Ref. 38 and shown in Figure 2a). The protocol consists of three steps:

1. The QD is set to the condition of Figure 1b) where there is an equal chance to have $n = 0$ and $n = 1$, which occurs for a doubly spin-degenerate energy level when $E = -k_B T \ln 2$.

2. A measurement of n is made. This provides one bit

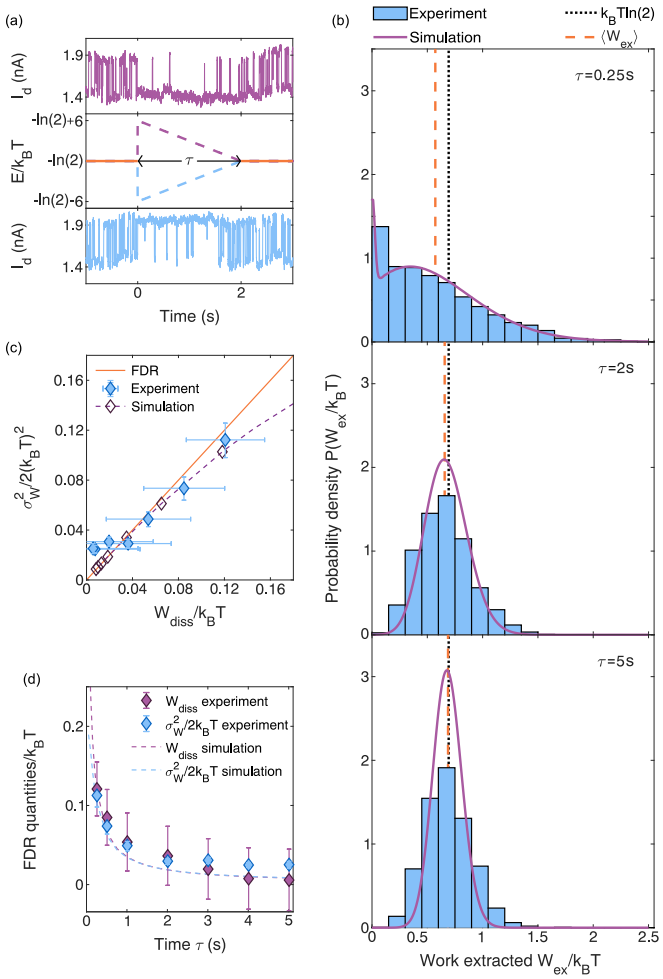


FIG. 2. a) The middle panel illustrates how the energy level is driven during the information-to-work conversion. Originally, it is offset from the reservoir Fermi level by $E = -k_BT\ln 2$. At time 0, a measurement is made. Depending on the outcome, the energy is rapidly driven either up or down by $6k_BT$ before slowly being driven back to the starting point. In this example, the protocol time $\tau = 2\,\mathrm{s}$. The upper (lower) panel shows the detector signal during one realization of the protocol where the energy was initially driven up (down). b) The distributions of extracted work for the Szilard engine operation for the protocol lengths $\tau = 0.25\,\mathrm{s}$ (top), 2 s (middle) and 5 s (bottom) together with the theoretically expected distribution (purple). The dotted black line indicates the Landauer limit $k_BT\ln 2$ and the orange dashed line indicates the mean extracted work. c) The two quantities from Eq. (1) plotted against each other. Here, $W_{\mathrm{diss}} = k_BT\ln 2 - \langle W\rangle$. The FDR line is Eq. (1), whereas the simulations are obtained by a full counting statistics method with Eq. (3). d) Same quantities as in c), but plotted against τ.

of information, which is used to extract work.

3. Depending on the measurement outcome, one of two feedback cycles is applied using V_{g1} (the top and bottom panels of Figure 2a) show example realizations of the two choices):

   (a) If $n = 0$, the level is rapidly raised by amplitude $A = +6k_BT$. This process does no work to the system as the energy level is empty. The energy level is then slowly ramped down to the starting point for a time τ, extracting at most $\langle W_{\mathrm{ex}}\rangle = k_BT\ln 2$.

   (b) If $n = 1$, the level is instead lowered by the drive amplitude, extracting $6k_BT$ of work and locking the state in $n = 1$. While ramping the energy back up, on average $\langle W\rangle \geq 6k_BT - k_BT\ln 2$ of work is performed to the system.

In both cases, the total amount of average work extracted in the cycle is bounded by $\langle W_{\mathrm{ex}}\rangle \leq k_BT\ln 2$. This limit can only be achieved in the ideal reversible limit, but finite-time implementations lead to both dissipation W_{diss} and fluctuations σ_W^2 as seen in the experimental data and supported by theory:

We consider the performance of the information-to-work protocol for different times τ, which we vary between 0.25 s and 5 s. Figure 2b) shows how the distribution of extracted work changes as τ is increased. In the short time limit, there is a large peak at $W_{\mathrm{ex}} = 0$ which arises from instances where no tunneling events had time to occur. As the drive is made slower, these cases become less likely and the distribution starts forming a Gaussian distribution approaching the Landauer limit $k_BT\ln 2$. As we approach this limit, the distribution also sharpens, and the work FDR also becomes valid, as demonstrated in Figs. 2c)-d) [1]: Figure 2c) shows the quantities of each side of Eq. (1) plotted against each other. The points line up with the diagonal, indicating that the work FDR does indeed hold. Furthermore, as seen in Figure 2d), both σ_W^2 and W_{diss} follow a $1/\tau$-dependence given by the analytical expression Eq. (5). In general, we observe very good agreement between theory and simulations. However, with largest τ's, σ_W^2 saturates in the experiment. This arises from offset charge drifts nearby QD1 that we observed to change at these time scales.

We now contrast the information-to-work conversion results with a protocol where no information is involved. The protocol is presented in Figure 3a). Like the Szilard engine case, it also starts at $E = -k_BT\ln 2$ with a 50% chance of QD1 being occupied. However, instead of making a measurement and quickly driving the level, it is slowly ramped down by the drive amplitude $2.5k_BT$ and then slowly ramped back up. On average, this protocol only creates dissipation since the initial and final states are the same, hence $\Delta F = 0$ in Eq. (2), which

[1] An important remark is that in order to study the work FDR, we focus only on instances where the correct feedback drive was applied. There is a possibility that an electron tunnels between the measurement is made and the feedback is applied, which gives rise to a second distribution centered around $k_BT(\ln 2 - 6)$. In this particular experiment, the error rate was roughly 3%, but we expect to see fewer errors if the device is run in a regime with slower tunnelling rates.

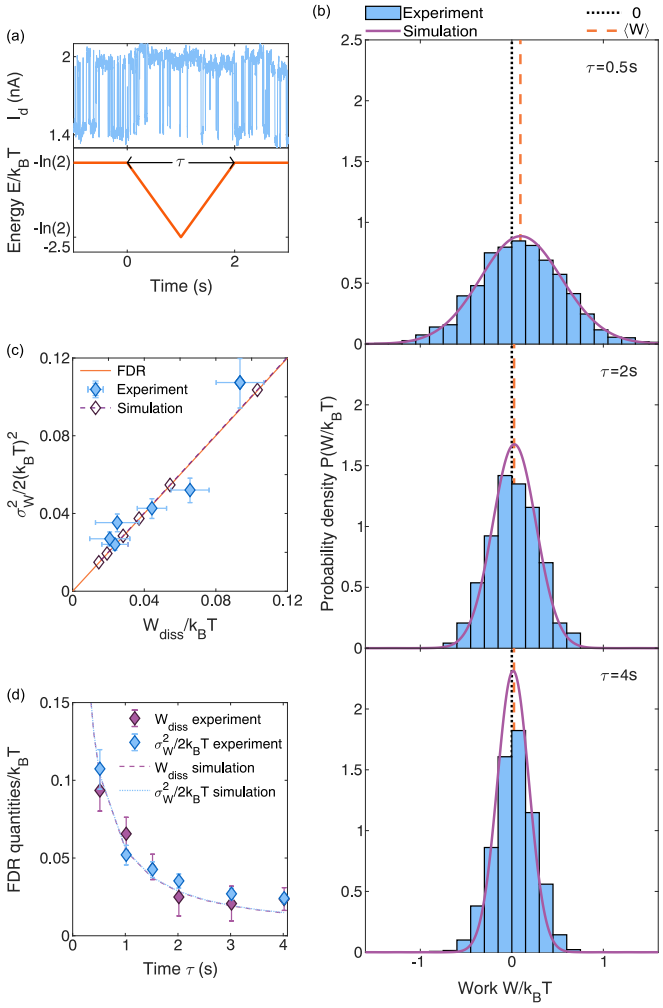


FIG. 3. a) Top panel: The detector signal I_d during the dissipative drive protocol, which is shown in the bottom panel. b) The work distribution of the $2.5k_BT$ dissipative drive for total protocol lengths 0.5 s (top), 2 s and 4 s (bottom) together with what is expected theoretically (purple). The orange line is the mean of the distribution which in this case is equal to W_{diss}. The black line is drawn at $W = 0$ to help guide the eye. c) The two sides of Eq. (1) plotted against each other, for protocol lengths between 0.5 s and 4 s. The orange diagonal is given by expression (5), which is obtained analytically in the slow-driving limit, and from which the FDR directly follows (see details in Appendix). d) The same quantities as in c), but now plotted against the protocol length.

is why we refer to it as the dissipative drive. In this case, $W_{\mathrm{diss}} = \langle W \rangle$. The drive period τ is varied between 0.5 s and 4 s, and Figure 3b) shows the work distribution in those limits as well as an intermediate case. It is clear that as the drive slows down, $\langle W \rangle \to 0$, while the distribution also sharpens up, in accordance with the FDR. The validity of the FDR for this cycle is shown in Figs. 3c-d), again finding very good agreement with experiment and theory expectations. Figure 4 summarizes the results for all protocols tested. This includes the previously discussed information-to-energy conversion drive

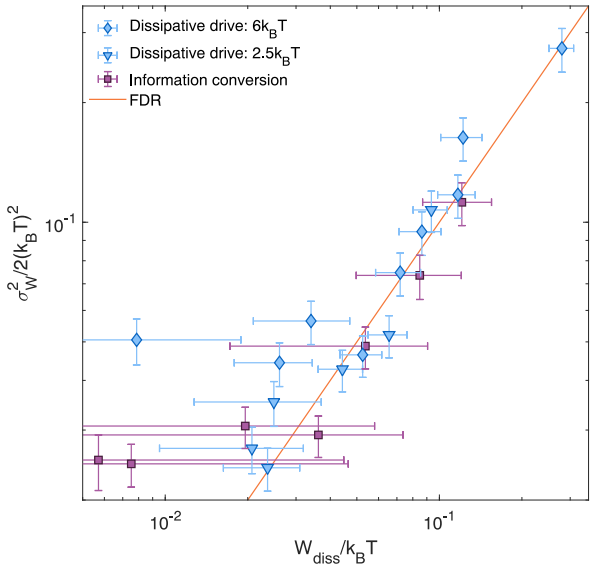


FIG. 4. The quantities in the work FDR in equation 1 plotted against each other for the information conversion protocol (purple) and the two dissipative protocols (blue, $6k_BT$ as diamonds and $2k_BT$ as triangles). To make the points easier to visually separate, the axes are logarithmic.

and the $2.5k_BT$ dissipative drive as well as an additional dissipative drive with a $6k_BT$ amplitude. All points follow Eq. (1), except the longest drives where the fluctuations saturate due to the offset charge drifts. These results encapsulate the main finding of this article: the experimental verification of the fundamental thermodynamic relation Eq. (1) at the level of a single-electron quantum dot.

Conclusions. In summary, we experimentally verified the work FDR for an information-to-work engine, implemented in a semiconductor quantum dot system. In agreement with the FDR, we observed a sharpening of the work distribution as the Landauer or reversible limit is approached. This implies that $k_BT \ln 2$ can be extracted almost *deterministically* from one bit of information (the electron's position in the dot). We contrasted these results with a process where no information about the electron was used. In this case, we also observed a decrease of dissipation accompanied by a decrease in fluctuations, but no work could be extracted on average.

Overall, our results highlight that the fundamental thermodynamic relation Eq. (1) is valid at the level of a single electron. These measurements constitute the first steps of studying information-to-work conversion using semiconductor quantum dots. Similar devices could be used to study, for instance, optimal protocols for information-to-work conversion [33, 55–59], as well as thermodynamic uncertainty relations [60]. Another future direction of interest is to, instead of inferring work output from the QD occupation, use information to generate a current and measure the work output directly [61].

Finally, a longer-term challenge is to experimentally show violations of the work FDR Eq. (1) due to the presence of quantum coherence, as theoretically predicted in Ref. 18.

Acknowledgments. We would like to thank Christopher Jarzynski for helpful discussions. D. B. and V. F. M. thank for financial support from NanoLund, Swedish Research Council, Foundational Questions Institute and the Knut and Alice Wallenberg Foundation (KAW) via Project No. 2016.0089. M. P.-L. acknowledges funding from Swiss National Science Foundation through an Ambizione grant PZ00P2-186067. M. S. acknowledges support from the European Union's Horizon 2020 research and innovation programme under the Marie Skłodowska-Curie grant agreement No 713729, and from the Government of Spain (FIS2020-TRANQI and Severo Ochoa CEX2019-000910- S), Fundacio Cellex, Fundació Mir-Puig, Generalitat de Catalunya (SGR 1381 and CERCA Programme).

[1] Christopher Jarzynski, "Equalities and inequalities: Irreversibility and the second law of thermodynamics at the nanoscale," Annual Review of Condensed Matter Physics **2**, 329–351 (2011).
[2] Udo Seifert, "Stochastic thermodynamics, fluctuation theorems and molecular machines," Reports on Progress in Physics **75**, 126001 (2012).
[3] Massimiliano Esposito, Upendra Harbola, and Shaul Mukamel, "Nonequilibrium fluctuations, fluctuation theorems, and counting statistics in quantum systems," Reviews of Modern Physics **81**, 1665–1702 (2009).
[4] Michele Campisi, Peter Hänggi, and Peter Talkner, "Erratum: Quantum fluctuation relations: Foundations and applications (Reviews of Modern Physics)," Rev. Mod. Phys. **83**, 771–791 (2011).
[5] John Goold, Marcus Huber, Arnau Riera, Lídia del Rio, and Paul Skrzypczyk, "The role of quantum information in thermodynamics—a topical review," Journal of Physics A: Mathematical and Theoretical **49**, 143001 (2016).
[6] J. Nulton, P. Salamon, B. Andresen, and Qi Anmin, "Quasistatic processes as step equilibrations," The Journal of Chemical Physics **83**, 334–338 (1985).
[7] Thomas Speck and Udo Seifert, "Distribution of work in isothermal nonequilibrium processes," Physical Review E **70**, 066112 (2004).
[8] Gavin E Crooks, "Measuring thermodynamic length." Phys. Rev. Lett. **99**, 100602 (2007).
[9] Johannes Hoppenau and Andreas Engel, "On the work distribution in quasi-static processes," Journal of Statistical Mechanics: Theory and Experiment **2013**, P06004 (2013).
[10] Chulan Kwon, Jae Dong Noh, and Hyunggyu Park, "Work fluctuations in a time-dependent harmonic potential: Rigorous results beyond the overdamped limit," Phys. Rev. E **88**, 062102 (2013).
[11] Marcus V. S. Bonança and Sebastian Deffner, "Optimal driving of isothermal processes close to equilibrium," The Journal of Chemical Physics **140**, 244119 (2014).
[12] Dibyendu Mandal and Christopher Jarzynski, "Analysis of slow transitions between nonequilibrium steady states," J. Stat. Mech. **2016**, 063204 (2016).
[13] Matteo Scandi, Harry J. D. Miller, Janet Anders, and Martí Perarnau-Llobet, "Quantum work statistics close to equilibrium," Phys. Rev. Research **2**, 023377 (2020).
[14] Bibek Bhandari, Pablo Terrén Alonso, Fabio Taddei, Felix von Oppen, Rosario Fazio, and Liliana Arrachea, "Geometric properties of adiabatic quantum thermal machines," Phys. Rev. B **102**, 155407 (2020).
[15] Jan Hermans, "Simple analysis of noise and hysteresis in (slow-growth) free energy simulations," J. Phys. Chem. **95**, 9029–9032 (1991), publisher: American Chemical Society.
[16] C. Jarzynski, "Nonequilibrium Equality for Free Energy Differences," Phys. Rev. Lett. **78**, 2690–2693 (1997), publisher: American Physical Society.
[17] Dibyendu Mandal and Christopher Jarzynski, "Analysis of slow transitions between nonequilibrium steady states," Journal of Statistical Mechanics: Theory and Experiment **2016**, 063204 (2016).
[18] Harry J. D. Miller, Matteo Scandi, Janet Anders, and Martí Perarnau-Llobet, "Work fluctuations in slow processes: Quantum signatures and optimal control," Phys. Rev. Lett. **123**, 230603 (2019).
[19] David A. Sivak and Gavin E. Crooks, "Thermodynamic Metrics and Optimal Paths," Physical Review Letters **108**, 190602 (2012).
[20] Gerhard Hummer, "Fast-growth thermodynamic integration: Error and efficiency analysis," The Journal of Chemical Physics **114**, 7330–7337 (2001).
[21] Christoph Dellago and Gerhard Hummer, "Computing equilibrium free energies using non-equilibrium molecular dynamics," Entropy **16**, 41–61 (2013).
[22] R. Landauer, "Irreversibility and Heat Generation in the Computing Process," IBM Journal of Research and Development **5**, 183–191 (1961), conference Name: IBM Journal of Research and Development.
[23] Rolf Landauer, "Dissipation and noise immunity in computation and communication," Nature **335**, 779–784 (1988).
[24] Takahiro Sagawa and Masahito Ueda, "Second law of thermodynamics with discrete quantum feedback control," Phys. Rev. Lett. **100**, 080403 (2008).
[25] Takahiro Sagawa and Masahito Ueda, "Generalized jarzynski equality under nonequilibrium feedback control," Phys. Rev. Lett. **104**, 090602 (2010).
[26] Jordan M. Horowitz and Juan M. R. Parrondo, "Thermodynamic reversibility in feedback processes," EPL (Europhysics Letters) **95**, 10005 (2011).
[27] Dibyendu Mandal and Christopher Jarzynski, "Work and information processing in a solvable model of maxwell's demon," Proceedings of the National Academy of Sciences **109**, 11641–11645 (2012).
[28] A. C. Barato and U. Seifert, "An autonomous and reversible maxwell's demon," EPL (Europhysics Letters) **101**, 60001 (2013).
[29] Sebastian Deffner and Christopher Jarzynski, "Information processing and the second law of thermodynamics: An inclusive, hamiltonian approach," Phys. Rev. X **3**, 041003 (2013).

[30] Juan M. R. Parrondo, Jordan M. Horowitz, and Takahiro Sagawa, "Thermodynamics of information," Nature Physics **11**, 131–139 (2015), number: 2 Publisher: Nature Publishing Group.

[31] Philippe Faist and Renato Renner, "Fundamental work cost of quantum processes," Phys. Rev. X **8**, 021011 (2018).

[32] Harry J. D. Miller, Giacomo Guarnieri, Mark T. Mitchison, and John Goold, "Quantum fluctuations hinder finite-time information erasure near the landauer limit," Phys. Rev. Lett. **125**, 160602 (2020).

[33] Karel Proesmans, Jannik Ehrich, and John Bechhoefer, "Finite-time landauer principle," Phys. Rev. Lett. **125**, 100602 (2020).

[34] Antoine Bérut, Artak Arakelyan, Artyom Petrosyan, Sergio Ciliberto, Raoul Dillenschneider, and Eric Lutz, "Experimental verification of Landauer's principle linking information and thermodynamics," Nature **483**, 187–189 (2012), number: 7388 Publisher: Nature Publishing Group.

[35] V. Serreli, CF. Lee, E. Kay, and D. A. Leigh, "A molecular information ratchet," Nature **445**, 523–527 (2007).

[36] Mark G. Raizen, "Comprehensive control of atomic motion," Science **324**, 1403–1406 (2009).

[37] Shoichi Toyabe, Takahiro Sagawa, Masahito Ueda, Eiro Muneyuki, and Masaki Sano, "Experimental demonstration of information-to-energy conversion and validation of the generalized Jarzynski equality," Nature Physics **6**, 988–992 (2010), number: 12 Publisher: Nature Publishing Group.

[38] Jonne V. Koski, Ville F. Maisi, Jukka P. Pekola, and Dmitri V. Averin, "Experimental realization of a Szilard engine with a single electron," PNAS **111**, 13786–13789 (2014), publisher: National Academy of Sciences Section: Physical Sciences.

[39] J. V. Koski, A. Kutvonen, I. M. Khaymovich, T. Ala-Nissila, and J. P. Pekola, "On-chip maxwell's demon as an information-powered refrigerator," Phys. Rev. Lett. **115**, 260602 (2015).

[40] Sebastian Lehmann, Jesper Wallentin, Daniel Jacobsson, Knut Deppert, and Kimberly A. Dick, "A general approach for sharp crystal phase switching in inas, gaas, inp, and gap nanowires using only group v flow," Nano Letters **13**, 4099–4105 (2013), pMID: 23902379, https://doi.org/10.1021/nl401554w.

[41] Malin Nilsson, Luna Namazi, Sebastian Lehmann, Martin Leijnse, Kimberly A. Dick, and Claes Thelander, "Single-electron transport in inas nanowire quantum dots formed by crystal phase engineering," Phys. Rev. B **93**, 195422 (2016).

[42] I-Ju Chen, Sebastian Lehmann, Malin Nilsson, Pyry Kivisaari, Heiner Linke, Kimberly A. Dick, and Claes Thelander, "Conduction band offset and polarization effects in inas nanowire polytype junctions," Nano Letters **17**, 902–908 (2017), pMID: 28002673, https://doi.org/10.1021/acs.nanolett.6b04211.

[43] D. Barker, S. Lehmann, L. Namazi, M. Nilsson, C. Thelander, K. A. Dick, and V. F. Maisi, "Individually addressable double quantum dots formed with nanowire polytypes and identified by epitaxial markers," Appl. Phys. Lett. **114**, 183502 (2019), publisher: American Institute of Physics.

[44] L. M. K. Vandersypen, J. M. Elzerman, R. N. Schouten, L. H. Willems van Beveren, R. Hanson, and L. P. Kouwenhoven, "Real-time detection of single-electron tunneling using a quantum point contact," Applied Physics Letters **85**, 4394–4396 (2004), https://aip.scitation.org/doi/pdf/10.1063/1.1815041.

[45] S. Gustavsson, R. Leturcq, M. Studer, I. Shorubalko, T. Ihn, K. Ensslin, D.C. Driscoll, and A.C. Gossard, "Electron counting in quantum dots," Surface Science Reports **64**, 191–232 (2009).

[46] Andrea Hofmann, Ville F. Maisi, Julien Basset, Christian Reichl, Werner Wegscheider, Thomas Ihn, Klaus Ensslin, and Christopher Jarzynski, "Heat dissipation and fluctuations in a driven quantum dot," physica status solidi (b) **254**, 1600546 (2017).

[47] A. Hofmann, V. F. Maisi, C. Rössler, J. Basset, T. Krähenmann, P. Märki, T. Ihn, K. Ensslin, C. Reichl, and W. Wegscheider, "Equilibrium free energy measurement of a confined electron driven out of equilibrium," Phys. Rev. B **93**, 035425 (2016).

[48] A. Hofmann, V. F. Maisi, C. Gold, T. Krähenmann, C. Rössler, J. Basset, P. Märki, C. Reichl, W. Wegscheider, K. Ensslin, and T. Ihn, "Measuring the degeneracy of discrete energy levels using a GaAs/AlGaAs quantum dot," Phys. Rev. Lett. **117**, 206803 (2016).

[49] Bjarne Andresen, Peter Salamon, and R. Stephen Berry, "Thermodynamics in finite time," Physics Today **37**, 62–70 (1984).

[50] Massimiliano Esposito, Ryoichi Kawai, Katja Lindenberg, and Christian Van den Broeck, "Efficiency at maximum power of low-dissipation carnot engines," Phys. Rev. Lett. **105**, 150603 (2010).

[51] A Calvo Hernández, A Medina, and J M M Roco, "Time, entropy generation, and optimization in low-dissipation heat devices," New Journal of Physics **17**, 075011 (2015).

[52] Viktor Holubec and Artem Ryabov, "Maximum efficiency of low-dissipation heat engines at arbitrary power," Journal of Statistical Mechanics: Theory and Experiment **2016**, 073204 (2016).

[53] Yu-Han Ma, Dazhi Xu, Hui Dong, and Chang-Pu Sun, "Universal constraint for efficiency and power of a low-dissipation heat engine," Phys. Rev. E **98**, 042112 (2018).

[54] Yu-Han Ma, Ruo-Xun Zhai, Jinfu Chen, C. P. Sun, and Hui Dong, "Experimental test of the $1/\tau$-scaling entropy generation in finite-time thermodynamics," Phys. Rev. Lett. **125**, 210601 (2020).

[55] Matteo Scandi and Martí Perarnau-Llobet, "Thermodynamic length in open quantum systems," Quantum **3**, 197 (2019).

[56] Paolo Abiuso, Harry J. D. Miller, Martí Perarnau-Llobet, and Matteo Scandi, "Geometric optimisation of quantum thermodynamic processes," Entropy **22**, 1076 (2020).

[57] Harry J. D. Miller and Mohammad Mehboudi, "Geometry of work fluctuations versus efficiency in microscopic thermal machines," Phys. Rev. Lett. **125**, 260602 (2020).

[58] Yi-Zheng Zhen, Dario Egloff, Kavan Modi, and Oscar Dahlsten, "Universal bound on energy cost of bit reset in finite time," arXiv preprint arXiv:2106.00580 (2021).

[59] Michael Konopik, Till Korten, Eric Lutz, and Heiner Linke, "Fundamental energy cost of finite-time computing," arXiv preprint arXiv:2101.07075 (2021).

[60] Patrick P. Potts and Peter Samuelsson, "Thermodynamic uncertainty relations including measurement and feedback," Phys. Rev. E **100**, 052137 (2019).

[61] Björn Annby-Andersson, Peter Samuelsson, Ville F. Maisi, and Patrick P. Potts, "Maxwell's demon in a

double quantum dot with continuous charge detection," Phys. Rev. B **101**, 165404 (2020).
[62] Vasco Cavina, Andrea Mari, and Vittorio Giovannetti, "Slow Dynamics and Thermodynamics of Open Quantum Systems," Physical Review Letters **119**, 050601 (2017).
[63] M. Campisi, S. Denisov, and P. Hänggi, "Geometric magnetism in open quantum systems," Phys. Rev. A **86**, 032114 (2012).
[64] S. Deffner and E. Lutz, "Thermodynamic length for far-from-equilibrium quantum systems," Phys. Rev. E **87**, 022143 (2013).
[65] María Florencia Ludovico, Francesca Battista, Felix von Oppen, and Liliana Arrachea, "Adiabatic response and quantum thermoelectrics for ac-driven quantum systems," Phys. Rev. B **93**, 075136 (2016).

Appendix A: Derivation of the FDR

For completeness, here we add a proof of the work FDR for the driven quantum dot. The results follow from the general considerations of Refs. 17, 18, but provide a more explicit derivation for the specific setting considered.

Recall that we consider a quantum dot with a two-fold degenerate energy level $E(t)$ that is driven for a time $t \in [0,\tau]$, which is in contact with a thermal fermionic reservoir. It is convenient to express the quantities of interest as $x_s \equiv x(s\tau)$ with $s \in (0,1)$. In terms of the renormalised variables, the equation of motion reads:

$$\frac{1}{\tau}\dot{p}_s = \Gamma_s(p_s^{\rm eq} - p_s) \tag{A1}$$

with $\dot{q}_s = \mathrm{d}q_s/\mathrm{d}s$, and where we introduced $\Gamma_s = \Gamma_0(1+bE_s)$ and $p_s^{\rm eq} = 1/(1+2e^{\beta(E_s)})$.

The stochastic variable $n_s \in \{0,1\}$ determines whether the dot is occupied or not at time $s\tau$. Hence, $\mathcal{E}[n_s] = p_s$ where $\mathcal{E}[.]$ denotes averaging over all trajectories. The work extracted in a given trajectory reads: $W = \int_0^\tau \mathrm{d}s\; n_s\dot{e}_s$. The average work is given by

$$\langle W\rangle = \mathcal{E}[W] = \int_0^1 \mathrm{d}s\; \mathcal{E}[n_s]\dot{E}_s = \int_0^1 \mathrm{d}s\; p_s\dot{E}_s. \tag{A2}$$

On the other hand, the work fluctuations read

$$\sigma_W^2 = \mathcal{E}[W^2] - (\mathcal{E}[W])^2 \tag{A3}$$

with $\mathcal{E}[W^2] = \int_0^1 \mathrm{d}s\;\int_0^1 \mathrm{d}t\; \mathcal{E}[n_s n_t]\dot{E}_s\dot{E}_t$. For $t \geq s$, $\mathcal{E}[n_s n_t]$ is given by $\mathcal{E}[n_s n_t] = p_s p_{t|s}$, where $p_{t|s}$ is the conditional probability of having $n_t = 1$ given that $n_s = 1$ at time $s < t$ (this ensures that the product $n_t n_s$ is non-zero). Hence we have $\mathcal{E}[W^2] = 2\int_0^\tau \mathrm{d}t\;\int_0^t \mathrm{d}s\; p_s p_{t|s}\dot{E}_s\dot{E}_t$, and also:

$$\sigma_W^2 = 2\int_0^\tau \mathrm{d}t\;\int_0^t \mathrm{d}s\; p_s(p_{t|s} - p_t)\dot{E}_s\dot{E}_t \tag{A4}$$

for the work fluctuations. In principle, both $\langle W\rangle$ and σ_W^2 can be computed exactly by solving the differential equation (A1). We obtain the formal solutions:

$$p_s = p_0 e^{-\tau\int_0^s \Gamma_y\,\mathrm{d}y} + \tau\int_0^s e^{-\tau\int_x^s \Gamma_y\,\mathrm{d}y}\Gamma_x p_x^{\rm eq}\,\mathrm{d}x. \tag{A5}$$

and

$$p_{t|s} = e^{-\tau\int_s^t \Gamma_y\,\mathrm{d}y} + \tau\int_s^t e^{-\tau\int_x^t \Gamma_y\,\mathrm{d}y}\Gamma_x p_x^{\rm eq}\,\mathrm{d}x. \tag{A6}$$

In order to obtain the FDR, we are interested in obtaining $\langle W\rangle$ and σ_W^2 analytically in the slow driving regime, i.e., at leading order in $1/\tau$. We proceed differently for each term. For $\langle W\rangle$, it is convenient to solve the differential equation (A1) perturbatively for $1/\tau$ by introducing the expansion: $p_s = p_s^{(0)} + \frac{1}{\tau}p_s^{(1)} + ...$ [62] (see also Refs. 56, 62–65). At zeroth order ($1/\tau = 0$), we simply find the equilibrium solution $p_s^{(0)} = p_s^{\rm eq}$. At first order, we have $p_s^{(1)} = -\dot{p}_s^{(0)}/\Gamma_s$, and hence:

$$\begin{aligned} p_s &= p_s^{\rm eq} - \frac{1}{\tau\Gamma_s}\dot{p}_s^{\rm eq} + \mathcal{O}\left(\frac{1}{\tau\Gamma_0}\right)^2 \\ &= p_s^{\rm eq} + \frac{\beta\dot{E}_s}{\tau\Gamma_s}(1-p_s^{\rm eq})p_s^{\rm eq} + \mathcal{O}\left(\frac{1}{\tau\Gamma_0}\right)^2 \end{aligned} \tag{A7}$$

where we used $p_s^{\rm eq} = 1/(1+2e^{\beta(E_s)})$ in the second line. Plugging this solution into (A2), we obtain:

$$\langle W \rangle = \Delta F + \frac{\beta}{\tau}\int_0^1 {\rm d}s\ (1-p_s^{\rm eq})p_s^{\rm eq}\frac{\dot{E}_s^2}{\Gamma_s} + \mathcal{O}\left(\frac{1}{\tau\Gamma_0}\right)^2 \tag{A8}$$

with $\Delta F = \int_0^1 {\rm d}s\ p_s^{\rm eq}\dot{E}_s$. Obtaining σ_W^2 at leading order in $1/\tau$ is more subtle, and we have to proceed differently. The underlying reason is that the perturbative solution (A7) disregards the memory of initial condition (which decays exponentially with time). This is well justified for p_s away from $s=0$, but not for $p_{t|s}$ where the regime $t \approx s$ is the most relevant one. Instead, we can expand directly the formal solution (A6) around $s=t$, obtaining at leading order:

$$\begin{aligned} p_{t|s} &= e^{-\tau\Gamma_t(t-s)} + \tau\int_s^t e^{-\tau\Gamma_t(t-x)}\Gamma_t p_t^{\rm eq}{\rm d}x + \mathcal{O}\left((t-s)e^{-\tau\Gamma_0(t-s)}\right) \\ &= p_t^{\rm eq} + e^{-\tau\Gamma_t(t-s)}(1-p_t^{\rm eq}) + \mathcal{O}\left((t-s)e^{-\tau\Gamma_0(t-s)}\right) \end{aligned} \tag{A9}$$

Plugging this expression into (A4), and consistently expanding around $s=t$, we obtain:

$$\begin{aligned} \sigma_W^2 &= 2\int_0^\tau {\rm d}t\ p_t^{\rm eq}(1-p_t^{\rm eq})\dot{E}_t^2\int_0^t \left[e^{-\tau\Gamma_t(t-s)} + \mathcal{O}\left((t-s)e^{-\tau\Gamma_0(t-s)}\right)\right]{\rm d}s \\ &= \frac{2}{\tau}\int_0^\tau {\rm d}t\ p_t^{\rm eq}(1-p_t^{\rm eq})\frac{\dot{E}_t^2}{\Gamma_t}\ + \mathcal{O}\left(\frac{1}{\tau\Gamma_0}\right)^2. \end{aligned} \tag{A10}$$

This provides the desired result:

$$W_{\rm diss} = \frac{\beta}{2}\sigma_W^2 + \mathcal{O}\left(\frac{1}{\tau\Gamma_0}\right)^2. \tag{A11}$$